Inorg. Chem. **2005**, *44*, 691–702

Copper(II) Complexes of a Series of Polypyridine Ligands Possessing a 1,2-Bis(2-pyridyl)ethane Common Moiety: Incorporation and Hydrolysis of Phosphate Esters

Motoharu Itoh, Jun Nakazawa, Kunihiro Maeda, Koji Kano, Tadashi Mizutani, and Masahito Kodera*

Department of Molecular Science and Technology, Doshisha University, Kyotanabe, Kyoto 610-0321, Japan

Received June 11, 2004

Two tetradentate ligands 1,2-bis[2-((dimethylamino)methyl)-6-pyridyl]ethane (L1) and 1,2-bis[2-(*N*-piperidinomethyl)-6-pyridyl]ethane (L2) and a hexadentate ligand 1,2-bis(2-((methyl(pyridylmethyl)amino)methyl)-6-pyridyl)ethane (L3) were prepared as part of a series of new polypyridine ligands possessing a 1,2-bis(2-pyridyl)ethane common moiety. L1 and L2 form mononuclear Cu(II) complexes $[Cu(L)(Cl)](ClO_4)$ [L = L1 (**1**) and L2 (**2**)], respectively. L3 forms a dinuclear Cu(II) complex $[Cu_2(L3)((PhO)_2PO_2)_2](ClO_4)_2$ (**3**) or a hexanuclear Cu(II) complex $[Cu_6(L3)_3((PhO)PO_3)_4](ClO_4)_4$ (**4**) in the presence of $(PhO)_2PO_2^-$ monoanion or $(PhO)PO_3^{2-}$ dianion, respectively. The structures of **1**–**4** were determined by X-ray analysis. The structures in solution were investigated by means of FAB and CSI MS spectrometers. The structural flexibility of the common 1,2-bis(2-pyridyl)ethane moiety and of the pendant groups allows complexes **1**–**4** to adapt to the various structures. Each Cu ion in **1** and **2** adopts a square pyramidal geometry with one Cl ion and two pendant groups (L1 and L2) binding in a bis-bidentate chelate mode. There is no steric repulsion between the pendant groups, so that the ligands specifically stabilize the mononuclear structures. L3 binds two Cu(II) ions with two pendant groups in tridentate chelate modes and, with the incorporation of phosphate esters, various dinuclear units are formed in **3** and **4**. In **4**, a dinuclear unit of $[Cu_2(L3)]^{4+}$ links two dinuclear units of $[Cu_2(L3)(PhOPO_3)_2]$ with four μ_3-1,3-$PhOPO_3^{2-}$ bridges. The hydrolytic activity of **2** and a dicopper(II) complex of L3 was examined with tris(*p*-nitrophenyl) phosphate (TNP) as a substrate.

Introduction

Polypyridine ligands have been extensively used to synthesize a variety of metal complexes[1] that possess unique polynuclear structures and functions in biomimetic systems.[2] 1,2-Bis[6-(2,2′-bipyridyl)]ethane (L4),[3] 1,2-bis[6-(6′-methyl-2,2′-pyridyl)]ethane (L5),[3] and 1,2-bis[2-(9-methyl-1,10-phenanthrolinyl)]ethane (L6)[3] are tetradenate ligands in which two 2,2′-bipyridines or two phenanthrolines at the α-positions of the N atoms are attached at both sides of a $-CH_2CH_2-$ spacer and where 1,2-bis(2-pyridyl)ethane is a common moiety (see Chart 1). L4 forms mononuclear[4] and dinuclear copper(II) complexes,[5] including various polynuclear metal complexes,[6] while L5 and L6 form dinuclear copper(I) complexes with double-strand helix structures.[7] The flexibility of the 1,2-bis(2-pyridyl)ethane moiety of L4−L6 essentially allows the various structures.

Chart 1. Structures of Tetradentate Ligands Having a 1,2-Bis(2-pyridyl)ethane Common Moiety

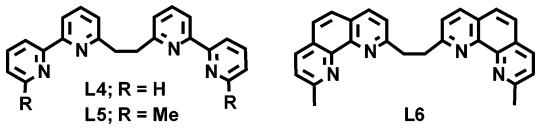

We have synthesized hexapyridine ligands,[8] in which two tripyridylmethane derivatives are attached at both sides of a $-CH_2CH_2-$ spacer and where 1,2-bis(2-pyridyl)ethane is a

* Author to whom correspondence should be addressed. E-mail: mkodera@mail.doshisha.ac.jp. Telephone: +81-774-65-6652. Fax: +81-774-65-6848.

(1) (a) Gavrilova, A. L.; Bosnich, B. *Chem. Rev.* **2004**, *104*, 349. (b) Kaes, C.; Katz, A.; Hosseini, M. W. *Chem. Rev.* **2000**, *100*, 3553.
(2) (a) Mirica, L. M.; Ottenwaelder, X.; Stack, T. D. P. *Chem. Rev.* **2004**, *104*, 1013. (b) Lewis, E. A.; Tolman, W. B. *Chem. Rev.* **2004**, *104*, 1047. (c) Molenveld, P.; Engbersen, J. F. J.; Reinhoudt, D. N. *Chem. Soc. Rev.* **2000**, *29*, 75.
(3) Lehn, J.-M.; Ziessel, R. *Helv. Chim. Acta* **1988**, *71*, 1511.
(4) Garber, T.; Wallendael, S. V.; Rillema, D. P.; Kirk, M.; Hatfield, W. E.; Welch, J. H.; Singh, P. *Inorg. Chem.* **1990**, *29*, 2863.
(5) Grant, C. M.; Stamper, B. J.; Knapp, M. J.; Folting, K.; Huffman, J. C.; Hendrickson, D. N.; Christou, G. *J. Chem. Soc., Dalton Trans.* **1999**, 3399.

10.1021/ic049240w CCC: $30.25
Published on Web 01/13/2005

Chart 2. Structures of Hexapyridine Ligands with a 1,2-Bis(2-pyridyl)ethane Common Moiety

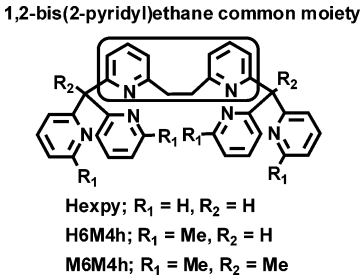

common moiety (see Chart 2). The hexapyridine ligands form stable dinuclear complexes that serve as useful structural and functional models of dimetal biosites.[8] The 1,2-bis(2-pyridyl)ethane moiety plays an essential role in stabilizing the dinuclear structures and in optimizing the distance between the two metal ions that possess several functions including O_2-binding and -activation.[9] Thus, the development of a variety of new polypyridine ligands possessing a 1,2-bis(2-pyridyl)ethane moiety that can serve as models of polymetal biosites is critical for increasing our basic understanding of these systems.

Dinuclear complexes bridged by phosphate esters are useful as models of alkaline phosphatase, a Zn-containing phosphomonoesterase that catalyzes the hydrolysis of a phosphate monoester using two cooperative Zn ions at the active center, such that the dizinc center binds a phosphate monoester in an O−P−O three atom bridging mode and no other bridging ligand is incorporated into the dizinc center.[10] In most of the model compounds reported so far, however, dinucleating ligands with an endogenous bridging group have been used to stabilize the dinuclear structures,[11] and as yet, only few examples are known concerning the stabilization

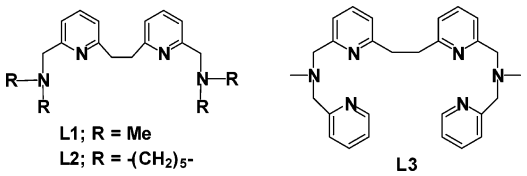

Figure 1. New tetra- and hexadentate ligands L1−L3 having a 1,2-bis-(2-pyridyl)ethane common moiety.

of a dinuclear structure using dinucleating ligands without an endogenous bridging group.[12] Polypyridine ligands possessing a 1,2-bis(2-pyridyl)ethane moiety may stabilize the dinuclear complexes bridged only by phosphate esters in the absence of any other bridging group as shown in the hexapyridine ligands.

In this study, two tetradentate ligands L1 and L2 and a hexadentate ligand L3 have been newly prepared. The chemical structures of L1−L3 are shown in Figure 1. To prepare L1−L3 we developed new synthetic routes with greatly improved yields, as compared with previous methods.[13] Either L1 or L2 binds a Cu(II) ion with two bidentate pendant groups to give the mononuclear complexes **1** or **2**, respectively. L3 binds two Cu(II) ions with two tridentate pendant groups and incorporates phosphate diesters and monoesters to afford the dinuclear and hexanuclear complexes **3** and **4**, respectively. To evaluate biological relevance, the hydrolytic activity of **2** and a dinuclear Cu(II) complex of L3 were examined with tris(*p*-nitrophenyl) phosphate as a substrate. Here, we report the syntheses of L1−L3 and their Cu(II) complexes **1**−**4**, the crystal structures of **1**−**4**, and the hydrolytic activity.

Experimental Section

Materials. All ordinary reagents and solvents were purchased and used as received unless otherwise noted. Tetrahydrofuran (THF) and diethyl ether (Et_2O) were dried over sodium metal and distilled. Absolute MeOH and EtOH were obtained by distillation over Mg. MeCN was dried over P_2O_5 and distilled. DMF was dried over CaH_2 and distilled under reduced pressure. 2-Bromo-6-picoline and 1,2-Bis(2-bromo-6-pyridyl)ethane were prepared according to reported methods.[7a]

(6) (a) Sanudo, E. C.; Grillo, V. A.; Yoo, J.; Huffman, J. C.; Bollinger, J. C.; Hendrickson, D. N.; Christou, G. *Polyhedron* **2001**, *20*, 1269. (b) Sanudo, E. C.; Grillo, V. A.; Knapp, M. J.; Bollinger, J. C.; Hendrickson, D. N.; Christou, G. *Inorg. Chem.* **2002**, *41*, 2441. (c) Grillo, V. A.; Sun, Z.; Folting, K.; Hendrickson, D. N.; Christou, G. *Chem. Commun.* **1996**, 2233. (d) Seddon, W. J.; Yoo, J.; Folting, K.; Huffman, J. C.; Hendrickson, D. N.; Christou, G. *J. Chem. Soc., Dalton Trans.* **2000**, 3640. (e) Grillo, V. A.; Knapp, M. J.; Bollinger, J. C.; Hendrickson, D. N.; Christou, G. *Angew. Chem., Int. Ed. Engl.* **1996**, *35*, 1818. (f) Grant, C. M.; Knapp, M. J.; Streib, W. E.; Huffman, J. C.; Hendrickson, D. N.; Christou, G. *Inorg. Chem.* **1998**, *37*, 6065.

(7) (a) Funeriu, D.-P.; He, Y.-B.; Bister, H.-J.; Lehn, J.-M. *Bull. Soc. Chim. Fr.* **1996**, *133*, 673. (b) Youinou, M.-T.; Ziessel, R.; Lehn, J.-M. *Inorg. Chem.* **1991**, *30*, 2144. (c) Shu, M.-H.; Duan, W.-Y.; Fu, Y.-J.; Zhang, W.-J.; Tang, W.-X. *J. Chem. Soc., Dalton Trans.* **1999**, 729.

(8) (a) Kodera, M.; Shimakoshi, H.; Nishimura, M.; Okawa, H.; Iijima, S.; Kano, K. *Inorg. Chem.* **1996**, *35*, 4967. (b) Kodera, M.; Katayama, K.; Tachi, Y.; Kano, K.; Hirota, S.; Fujinami, S.; Suzuki, M. *J. Am. Chem. Soc.* **1999**, *121*, 11006. (c) Kodera, M.; Kajita, Y.; Tachi, Y.; Katayama, K.; Kano, K.; Hirota, S.; Fujinami, S.; Suzuki, M. *Angew. Chem., Int. Ed.* **2004**, *43*, 334.

(9) (a) Kodera, M.; Shimakoshi, H.; Tachi, Y.; Katayama, K.; Kano, K. *Chem. Lett.* **1998**, 441. (b) Kodera, M.; Tachi, Y.; Hirota, S.; Katayama, K.; Shimakoshi, H.; Kano, K.; Fujisawa, K.; Moro-oka, Y.; Naruta, Y.; Kitagawa, T. *Chem. Lett.* **1998**, 389. (c) Kodera, M.; Taniike, Y.; Itoh, M.; Tanahashi, Y.; Shimakoshi, H.; Kano, K.; Hirota, S.; Iijima, S.; Ohba, M.; Okawa, H. *Inorg. Chem.* **2001**, *40*, 4821. (d) Kodera, M.; Shimakoshi, H.; Kano, K. *Chem. Commun.* **1996**, 1737.

(10) (a) Kim, E. E.; Wyckoff, H. W. *J. Mol. Biol.* **1991**, *218*, 449. (b) Stec, B.; Holtz, K. M.; Kantrowitz, E. R. *J. Mol. Biol.* **2000**, *299*, 1303.

(11) (a) Wall, M.; Hynes, R. C.; Chin, J. *Angew. Chem.* **1993**, *105*, 1696. (b) Gajda, T.; Krámer, R.; Jancsó, A. *Eur. J. Inorg. Chem.* **2000**, 1635. (c) Gajda, T.; Jancsó, A.; Mikkola, S.; Lönnberg, H.; Sirges, H. *J. Chem. Soc., Dalton Trans.* **2002**, 1757. (d) Yun, J. W.; Tanase, T.; Pence, L. E.; Lippard, S. J. *J. Am. Chem. Soc.* **1995**, *117*, 4407. (e) Albedyhl, S.; Averbuch-Pouchot, M. T.; Belle, C.; Krebs, B.; Pierre, J. L.; Saint-Aman, E.; Torelli, S. *Eur. J. Inorg. Chem.* **2001**, 1457. (f) Yin, L.-H.; Cheng, P.; Yan, S.-P.; Fu, X.-Q.; Li, J.; Liao, D.-Z.; Jiang, Z.-H. *J. Chem. Soc., Dalton Trans.* **2001**, 1398. (g) Yamaguchi, K.; Akagi, F.; Fujinami, S.; Suzuki, M.; Shionoya, M.; Suzuki, S. *Chem. Commun.* **2001**, 375. (h) Seo, J. S.; Hynes, R. C.; Williams, D.; Chin, J. *J. Am. Chem. Soc.* **1998**, *120*, 9943. (i) Koike, T.; Inoue, M.; Kimura, E.; Shiro, M. *J. Am. Chem. Soc.* **1996**, *118*, 3091. (j) Yun, J. W.; Tanase, T.; Lippard, S. J. *Inorg. Chem.* **1996**, *35*, 7590. (k) Tanase, T.; Yun, J. W.; Lippard, S. J. *Inorg. Chem.* **1996**, *35*, 3585. (l) Kinoshita, E.; Takahashi, M.; Takeda, H.; Shiro, M.; Koike, T. *Dalton Trans.* **2004**, 1189.

(12) (a) Williams, N. H.; Takasaki, B.; Wall, M.; Chin, J. *Acc. Chem. Res.* **1999**, *32*, 485. (b) Bazzicalupi, C.; Bencini, A.; Bianchi, A.; Fusi, V.; Giorgi, C.; Paoletti, P.; Valtancoli, B.; Zanchi, D. *Inorg. Chem.* **1997**, *36*, 2784.

(13) (a) Jones, G.; Mouat, D. J.; Tonkinson, D. J. *J. Chem. Soc., Perkin Trans. 1* **1985**, 2719. (b) Baker, W.; Buggle, K. M.; McOmie, J. F. W.; Watkins, D. A. M. *J. Chem. Soc.* **1958**, 3594.

Measurements. Elemental analyses (C, H, and N) were carried out at the Elemental Analysis Service Center of Kyoto University. The amount of copper was determined using a Shimazu AA-610 atomic absorption/flame emission spectrophotometer. UV−vis absorption spectra were recorded on a Hitachi U-3210 spectrophotometer and an Oothuka Photal MCPD-7000 MM. Infrared (IR) spectra were taken on a Shimadzu FT IR-8400 spectrometer using KBr disks or NaCl plates. Fast atom bombardment (FAB) mass spectra were obtained on a JEOL JMS-DX 300 spectrometer using *m*-nitrobenzyl alcohol (NBA) as a matrix. Cold spray ionization (CSI) mass spectrum were obtained on a JEOL JMS-T100CS spectrometer in MeCN at −30 °C and in 30% MeCN/H_2O (v/v) at 5 °C. ^{1}H NMR spectra in $CDCl_3$ and D_2O were recorded on a JEOL JMN-A 400 spectrometer using Me_4Si and sodium (trimethylsilyl)-propionate-d_4 (TSP) as internal standards. ESR spectra were recorded on a JEOL JES-TE200 spectrometer in MeCN or MeCN−CH_2Cl_2 at 77 K.

Preparations. 1,2-Bis(2-formyl-6-pyridyl)ethane. In dry THF (350 mL) was dissolved 1,2-bis(2-bromo-6-pyridyl)ethane (5.12 g, 0.015 mol) and the mixture degassed by evacuation and subsequent refilling with Ar. To the solution was added *n*-butyllithium (1.6 M in hexane, 20 mL, 0.032 mol) at −78 °C. The solution was kept at −78 °C and stirred for 1 h under Ar. To the solution was added dropwise DMF (4 mL, 0.05 mol) in 48 mL of dry Et_2O. The mixture was warmed to room temperature and stirred for 5 h under Ar. To the resultant mixture was added 2 M aqueous HCl (40 mL), and THF was removed by evaporation. To the residue was added 200 mL of $CHCl_3$ and 100 mL of distilled water, and this mixture was neutralized with Na_2CO_3. The $CHCl_3$ layer was separated, and the aqueous layer was extracted with $CHCl_3$ (100 mL × 2). The $CHCl_3$ layers were combined, dried over anhydrous Na_2SO_4, and concentrated to dryness to afford crude products in the form of a brown solid. 1,2-Bis(2-formyl-6-pyridyl)ethane was purified by recrystallization from CH_2Cl_2 (3.08 g, yield 85.6%): mp 189−191 °C (lit.[13a] mp 181−183 °C). FT-IR data (ν/cm^{-1}) on KBr disks: 3100 (aromatic C−H), 2825 (aldehyde C−H), 1695 (carboxyl C═O), and 1585 and 1455 (aromatic ring). ^{1}H NMR data (δ/ppm vs Me_4-Si) in $CDCl_3$: 3.43 (4H, s, $-CH_2-$), 7.32 (2H, d, H_{py-5}), 7.74 (2H, d, H_{py-3}), 7.80 (2H, t, H_{py-4}), and 10.06 (2H, s, −CHO). FAB MS data: *m*/*z* 241, $[M + H]^+$.

1,2-Bis(2-(hydroxymethyl)-6-pyridyl)ethane. In THF (30 mL) and water (5 mL) was dissolved 1,2-bis(2-formyl-6-pyridyl)ethane (0.4 g, 0.001 67 mol). To the solution was added $NaBH_4$ (0.13 g, 0.003 42 mol) at room temperature. The solution was acidified with concentrated HCl to pH 2, and THF was removed by distillation. To the residue were added 200 mL of $CHCl_3$ and 100 mL of distilled water, and this mixture was neutralized with Na_2CO_3. The $CHCl_3$ layer was separated, and the aqueous layer was extracted with $CHCl_3$ (100 mL × 2). The $CHCl_3$ layers were combined, dried over anhydrous Na_2SO_4, and concentrated to dryness to afford a white solid. The solid was recrystallized from CH_2Cl_2 (0.4 g, yield 98%): mp 157−159 °C (lit.[13b] mp 157−159 °C). FT-IR data (ν/cm^{-1}) on KBr disks: 3450 (−OH), 3100 (aromatic C−H), 2850, 2800 (aliphatic C−H), and 1590, 1570, 1450, and 1430 (aromatic ring). ^{1}H NMR data (δ/ppm vs Me_4Si) in $CDCl_3$: 3.28 (4H, s, $-CH_2-$), 4.10 (2H, s, −OH), 4.72 (4H, s, $-CH_2OH$), 7.03 (4H, m, $H_{py-3\ and\ 5}$), and 7.56 (2H, t, H_{py-4}). FAB MS data: *m*/*z* 245, $[M + H]^+$.

1,2-Bis(6-(bromomethyl)-2-pyridyl)ethane·2HBr. 1,2-Bis(6-(bromomethyl)-2-pyridyl)ethane ·2HBr (yield 94%) was prepared from 1,2-bis(2-(hydroxymethyl)-6-pyridyl)ethane essentially as reported elsewhere.[13b] The yield of the product was improved by using a small amount of ethyl acetate as a washing solvent: mp 118−120 °C [lit.[13b] mp 118−120 °C (dec)]. FT-IR data (ν/cm^{-1}) on KBr disks: 3094 and 3055 (aromatic C−H), 2978, 2899, and 2862 (aliphatic C−H), and 1674, 1636, and 1620 (aromatic ring). ^{1}H NMR data (δ/ppm vs TSP) in D_2O: 3.43 (4H, s, $-CH_2-$), 4.63 (4H, s, $-CH_2Br$), 7.65 (2H, d, H_{py-3}), 7.80 (2H, d, H_{py-5}), and 8.27 (2H, t, H_{py-4}). FAB MS data: *m*/*z* 371, $[M - 2HBr + H]^+$.

1,2-Bis[2-((dimethylamino)methyl)-6-pyridyl]ethane·4HCl (L1·4HCl). In a 50% aqueous solution of dimethylamine (10 mL) was dissolved 1,2-bis(2-(bromomethyl)-6-pyridyl)ethane·2HBr (100 mg, 0.19 mmol) and the mixture stirred for 12 h at room temperature. Excess dimethylamine was removed by distillation. The solution was acidified with concentrated HCl to pH 2 and concentrated to dryness, and the solid was washed with acetone (yield 75.1 mg, 89%): mp 234−237 °C (dec). Anal. Calcd for $C_{18}H_{36}N_4O_3Cl_4$: C, 43.38; H, 7.28; N, 11.24. Found: C, 43.77; H, 6.99; N, 11.34. FT-IR data (ν/cm^{-1}) on KBr disks: 3040 and 3010 (aromatic C−H), 2910 (aliphatic C−H), 2690 (N^{+-}H), and 1680, 1620, and 1480 (aromatic ring). ^{1}H NMR data (δ/ppm vs TSP) in D_2O: 2.93 (12H, s, $N-CH_3$), 3.37 (4H, s, py$-CH_2-$N), 4.49 (4H, s, py$-CH_2CH_2-$py), 7.48 (2H, d, H_{py-5}), 7.56 (2H, d, H_{py-3}), and 7.99 (2H, t, H_{py-4}). FAB MS data: *m*/*z* 299, $[M + H]^+$.

1,2-Bis[2-(*N*-piperidinomethyl)-6-pyridyl]ethane·4HCl (L2·4HCl). In MeOH (20 mL) was added 1,2-bis(2-(bromomethyl)-6-pyridyl)ethane·2HBr (100 mg, 0.19 mmol) and piperidine (4 mL) and the mixture stirred for 12 h. Excess piperidine was removed by distillation. The solution was acidfied with concentrated HCl to pH 2 and concentrated to dryness, and the solid was washed with acetone (yield 68 mg, 62%): mp 255−257 °C (dec). Anal. Calcd for $C_{24}H_{43}N_4Cl_4O_{2.5}$: C, 50.62; H, 7.61; N, 9.84. Found: C, 50.57; H, 7.43; N, 9.75. FT-IR data (ν/cm^{-1}) on KBr disks: 3010 (aromatic C−H), 2930 and 2850 (aliphatic C−H), and 1640, 1620, 1590, 1570, and 1455 (aromatic ring). ^{1}H NMR data (δ/ppm vs TSP) in D_2O: 1.45 (4H, m, pip-4), 1.61 (8H, m, pip-3,5), 2.45 (8H, m, pip-2,6), 3.20 (4H, s, py$-CH_2CH_2-$py), 3.63 (4H, s, py$-CH_2-$N), 6.97 (2H, d, H_{py-5}), 7.26 (2H, d, H_{py-3}), and 7.51 (2H, t, H_{py-4}). FAB MS data: *m*/*z* 379, $[M + H]^+$.

1,2-Bis(2-(((pyridylmethyl)amino)methyl)-6-pyridyl)ethane. In 30 mL of MeOH was added 1,2-bis(2-formyl-6-pyridyl)ethane (300 mg, 1.25 mmol) and fleshly distilled 2-(aminomethyl)pyridine (300 mg, 2.77 mmol) and the mixture allowed to react for 1 h. Following concentration of the reaction mixture to 10 mL, $NaBH_4$ (190 mg, 5 mmol) was added and the mixture was stirred for 12 h. The reaction mixture was then acidified with concentrated HCl to pH 1, and solid was precipitated. Following removal of the solid by filtration, the filtrate was concentrated to afford a brown oily reside. To the oily residue was added CH_2Cl_2 (100 mL) and an aqueous solution of NaOH. The CH_2Cl_2 layer was separated and concentrated to afford an oily residue (500 mg, yield 94%). FT-IR data (ν/cm^{-1}) on NaCl plate: 3310 (−NH), 3060 (aromatic C−H), 2920 and 2850 (aliphatic C−H), and 1590, 1570, and 1450 (aromatic ring). ^{1}H NMR data (δ/ppm vs Me_4Si) in $CDCl_3$: 2.48 (2H, br, NH), 3.22 (4H, s, py$-CH_2CH_2-$py), 3.95 (4H, s, $-CH_2-$py$-CH_2-$N), 3.98 (4H, s, py′$-CH_2-$N), 6.99 (2H, d, H_{py-5}), 7.15 (4H, d−d, $H_{py-3\ and\ py'-5}$), 7.38 (2H, d, $H_{py'-3}$), 7.49 (2H, t, H_{py-4}), 7.65 (2H, t, $H_{py'-4}$), and 8.56 (2H, d, $H_{py'-6}$). FAB MS data: *m*/*z* 425, $[M + H]^+$.

1,2-Bis(2-((methyl(pyridylmethyl)amino)methyl)-6-pyridyl)-ethane (L3). To a mixture of formic acid (1 mL), formalin (1 mL), and H_2O (1 mL) was added 1,2-bis(2-(((pyridylmethyl)amino)-methyl)-6-pyridyl)ethane (240 mg, 0.57 mmol), and the solution was refluxed with vigorous stirring for 12 h. Following concentration of the resultant mixture to dryness, Et_2O (100 mL) and aqueous NaOH were added. The Et_2O layer was separated and

concentrated to afford a yellow oily residue (210 mg, yield 81.5%). FT-IR data (ν/cm^{-1}) on NaCl plate: 3059 and 3009 (aromatic C−H), 2928, 2839, and 2795 (aliphatic C−H), and 1676, 1572, and 1433 (aromatic ring). ^{1}H NMR data (δ/ppm vs Me_4Si) in $CDCl_3$: 2.31 (6H, s, NCH_3), 3.21 (4H, s, py−CH_2CH_2−py), 3.76 (8H, s, py−CH_2−N−CH_2−py′), 6.98 (2H, d, H_{py-5}), 7.16 (4H, m, $H_{py-3\ and\ py'-3}$), 7.33 (2H, d, $H_{py'-5}$), 7.51 (2H, t, $H_{py'-4}$), 7.65 (2H, t, H_{py-4}), and 8.56 (2H, d, $H_{py'-6}$). FAB MS data: m/z 453, [M + H]$^+$.

Synthesis of Copper(II) Complexes. [Cu(L1)(Cl)](ClO$_4$) (1). To 1.0 mL of MeOH was added L1·4HCl (16.9 mg, 0.038 mmol) and $Cu(ClO_4)_2$·$6H_2O$ (14.0 mg, 0.038 mmol) and the solution neutralized by the addition of NaOH. The mixture was stirred for 3 h at room temperature and concentrated to 0.3 mL. To the residue was added Et_2O to afford a blue solid (17 mg, yield 90%), and blue crystals suitable for X-ray structure analysis were obtained by recrystallization from a solution in MeOH by slow evaporation. Anal. Calcd for $C_{18}H_{26}N_4O_4CuCl_2$: C, 43.51; H, 5.27; N, 11.28, Cu, 12.79. Found: C, 42.41; H, 5.23; N, 11.02; Cu, 12.49. UV−vis absorption property in CH_3CN [λ_{max}/nm (ϵ_{max}/dm^3 mol^{-1} cm^{-1})]: 270 (14 000), 730 (240). FT-IR data (ν/cm^{-1}) on KBr disks: 3000 (aromatic C−H), 2950 and 2900 (aliphatic C−H), 1600 and 1470 (aromatic ring), and 1080 (ClO_4). FAB MS data (m/z): 496, [M + H]$^+$; 461, [M − Cl]$^+$; 396, [M − ClO_4]$^+$. ESR (77K): $g_\perp = 2.09$, $g_{||} = 2.23$, $A_{||} = 127$ G.

[Cu(L2)(Cl)](ClO$_4$) (2). **2** (yield 86%) was synthesized essentially as described for **1** using L2·4HCl in place of L1·4HCl, and blue crystals suitable for X-ray structure analysis were obtained by recrystallization from a solution in MeOH by slow evaporation. Anal. Calcd for $C_{25}H_{36}N_4O_4CuCl_2$: C, 50.80; H, 6.14; N, 9.48; Cu, 10.75. Found: C, 49.75; H, 5.73; N, 9.66; Cu, 10.11. UV−vis absorption property in CH_3CN [λ_{max}/nm (ϵ_{max}/dm^3 mol^{-1} cm^{-1})]: 270 (9600), 750 (170). FT-IR data (ν/cm^{-1}) on KBr disks: 3080 (aromatic C−H), 2935 and 2860 (aliphatic C−H), 1620 and 1460 (aromatic ring), and 1090 (ClO_4). FAB MS data (m/z): 539, [M −Cl]$^+$; 441, [M − Cl − ClO_4]$^+$. ESR (77K): $g_\perp = 2.08$, $g_{||} = 2.23$, $A_{||} = 134$ G.

[Cu$_2$(L3)((PhO)$_2$PO$_2$)$_2$](ClO$_4$)$_2$ (3). To 10 mL of MeOH was added L3 (60 mg, 0.133 mmol) and $Cu(ClO_4)_2$·$6H_2O$ (100 mg, 0.27 mmol) and the mixture stirred for 10 min. Following the addition of $Na(PhO)_2PO_2$ (45 mg, 0.17 mmol), the mixture was stirred for 1 h and then Et_2O was slowly added which resulted in the precipitation of a green solid. The solid was collected by filtration and dissolved in CH_2Cl_2, and insoluble materials were removed by filtration. The filtrate was concentrated to dryness to afford a crude green solid. This was purified by recrystallization from MeCN−CH_2Cl_2−1,2-dimethoxyethane to afford green crystals (45 mg, yield 42%) suitable for X-ray analysis. Anal. Calcd for $C_{52}H_{52}N_6O_{16}Cl_2Cu_2P_2$: C, 48.91; H, 4.10; N, 6.58; Cu, 9.95. Found: C, 48.50; H, 4.06; N, 6.48; Cu, 9.71. UV−vis absorption property in CH_3CN [λ_{max}/nm (ϵ_{max}/dm^3 mol^{-1} cm^{-1})]: 260 (26 000), 710 (160). FT-IR data (ν/cm^{-1}) on KBr disks: 3040 (aromatic C−H), 2920 (aliphatic C−H), 1605, 1590, and 1490 (aromatic ring), and 1085 (ClO_4). FAB MS data (m/z): 1175, [M − ClO_4]$^+$; 1076, [M − 2ClO_4]$^+$; 926, [M − $(PhO)_2PO_2$ − ClO_4]$^+$. ESR (77 K): g = 2.13 (broad).

Dicopper(II) Complex of L3 for the Kinetic Studies. To 3 mL of 30% MeCN−H_2O (3:7 MeCN−H_2O, v/v) buffer solution of 4.0 mM $Cu(ClO_4)_2$·$6H_2O$ was added L3 (2.72 mg, 6.00 mmol) and the mixture stirred for 1 h. The formation of dicopper(II) complex was confirmed by the increase at 710 nm. The structures of the generated dicopper(II) complexes at various pHs were examined by CSI mass spectra (see Figure 6).

[Cu$_6$(L3)$_3$(PhOPO$_3$)$_4$](ClO$_4$)$_4$ (4). To 10 mL of MeOH was added L3 (60 mg, 0.133 mmol) and $Cu(ClO_4)_2$·$6H_2O$ (100 mg, 0.27 mmol) and the mixture stirred for 10 min. To this was then added Na_2PhOPO_3 (100 mg, 0.39 mmol) and the mixture stirred for an additional 1 h. The green solid that had precipitated was collected by filtration and recrystallized from MeCN−CH_2Cl_2−Et_2O to afford blue crystals (73 mg, yield 56%) suitable for X-ray analysis. Anal. Calcd for $C_{108}H_{126}Cl_4N_{18}O_{37}P_4Cu_6$: C, 44.50; H, 4.36; N, 8.65; Cu, 13.08. Found: C, 44.98; H, 4.07; N, 8.81; Cu, 12.61. UV−vis absorption property in CH_3CN [λ_{max}/nm (ϵ_{max}/dm^3 mol^{-1} cm^{-1})]: 260 (65 000), 710 (440). FT-IR data (ν/cm^{-1}) on KBr disks: 3050 (aromatic C−H), 2925 (aliphatic C−H), 1610, 1575, and 1490 (aromatic ring), and 1085 (ClO_4). FAB MS data (m/z): 1084, [L3 + 3Cu + 2(PhO)PO_3 + ClO_4]$^+$; 985, [L3 + 3Cu + 2(PhO)PO_3]$^+$; 945, [L3 + 2Cu + 2(PhO)PO_3 + Na]$^+$; 923, [L3 + 2Cu + 2(PhO)-PO_3 + H]$^+$; 750, [L3 + 2Cu + (PhO)PO_3]$^+$; 515, [L3 + Cu]$^+$. ESR (77 K): g = 2.12 (broad).

Kinetics of Tris(*p*-nitrophenyl) Phosphate Hydrolysis. The hydrolysis of tris(*p*-nitrophenyl) phosphate (TNP) in 30% MeCN−H_2O solution (3:7 MeCN−H_2O, v/v) was followed by an increase in absorption maximum at 400 nm for generation of *p*-nitrophenolate ion at 35 ± 0.5 °C and I = 0.10 ($NaClO_4$). All rate measurements were performed under pseudo-first-order conditions of excess Cu(II) complex. Buffer solutions were prepared with HEPES (pH 7−8), TAPS (pH 8−9), and CHES (pH > 9), and the pH was exactly adjusted by using NaOH (0.20−2.00 mM). A typical procedure for the kinetic experiment is as follows: A 30% MeCN−H_2O buffer solution (0.5 mL, 20 mM CHES, pH 9) of the Cu(II) complex was placed in a 2 mm quartz cell, and to the solution was added 5 μL of 2.0 mM TNP in dry THF by using a microsyringe. After the solution was rapidly mixed, the absorption increase was recorded until 90% hydrolysis was completed; an end point was determined after >5$t_{1/2}$. The succeeding hydrolysis of the generated bis(*p*-ntrophenyl) phosphate was too slow to be detected under these conditions. The pseudo-first-order rate constants, k_{obs} (s^{-1}), were obtained from fits of $-\ln(1 - A_t/A_\infty)$ vs time. A plot of the kinetic data gave straight lines in each kinetic measurement. Several reference experiments were carried out where similar reaction conditions were used except that the Cu(II) complex was not contained.

Structure Determination of Single Crystals. The crystal structures of **1**−**4** were determined using a Rigaku AFC7R/CCD diffractometer with graphite-monochromated Mo Kα radiation (λ = 0.710 69) and a 12 kW rotating anode generator. The data were collected at 293 ± 1 and 223 ± 1 K to a maximum 2θ value of 55.0°. A total of 660 oscillation images for **1**−**3** were collected. A sweep of data was performed using a ϕ scan from −80.0 to 100.0° in 0.5° steps, at ω = 0.0° and χ = 0.0°. The detector swing angle was 9.80−10.05°. A second sweep was performed using ω scans from −30.0 to 20.0° in 0.5° steps, at ω = 90.0° and χ = 0.0°. The detector swing angle was 9.80−10.05°. A further sweep was performed using ω scans from −30.0 to 20.0° in 0.5° steps, at ω = 90.0° and χ = 90.0°. The detector swing angle was 9.80−10.05°. An additional sweep was performed using ω scans from −30.0 to 20.0° in 0.5° steps, at ω = 90.0° and χ = 180.0°. The detector swing angle was 9.80−10.05°. The crystal-to-detector distance was 35.02 mm. Readout was performed in the 0.273 mm pixel mode.

A total of 1240 oscillation images for **4** were collected. A sweep of data was done using a ϕ scan from −80.0 to 100.0° in 0.3° steps, at ω = 0.0° and χ = 0.0°. The detector swing angle was 19.91°. A second sweep was performed using ω scans from −20.0 to 28.0° in 0.3° steps, at ω = 90.0° and χ = 0.0°. The detector swing angle was 19.91°. Another sweep was performed using ω

Table 1. Crystallographic Data for 1−4

	1	2	3	4
formula	$C_{18}H_{26}N_4O_4Cl_2Cu$	$C_{26}H_{37}N_5O_4Cl_2Cu$	$C_{52}H_{52}N_6O_{16}Cl_2P_2Cu_2$	$C_{108}H_{132}N_{18}O_{40}Cl_4P_4Cu_6$
fw	496.88	618.06	1276.96	2967.29
cryst syst	monoclinic	monoclinic	monoclinic	monoclinic
space group	$P2_1/c$ (No. 14)	$P2_1/c$ (No. 14)	$P2_1/n$ (No. 14)	$P2_1/c$ (No. 14)
a/Å	11.588(2)	12.043(2)	17.277(4)	18.221(4)
b/Å	14.246(2)	14.211(2)	18.549(4)	39.832(10)
c/Å	13.297(2)	16.888(3)	17.418(4)	22.519(9)
β/deg	100.108(3)	101.515(3)	95.357(5)	96.844(4)
V/Å^3	2161.2(6)	2832.0(7)	5557.4(20)	16226.8(69)
Z	4	4	4	4
T/°C	−50	−50	−50	−50
D_c/g cm^{-3}	1.527	1.449	1.526	1.215
radiatn (λ)/Å	Mo Kα (0.710 70)	Mo Kα (0.710 70)	Mo Kα (0.710 70)	Mo Kα (0.710 70)
μ/cm^{-1}	12.89	10.01	9.93	9.47
R, R_w[a]	0.034, 0.048	0.072, 0.131	0.076, 0.105	0.108, 0.126
GOF index	1.004	0.941	1.000	1.699

[a] $R = \sum||F_o| - |F_c||/\Sigma|F_o|$. $R_w = [\sum w(|F_o| - |F_c|)^2/\sum w(F_o)^2]^{1/2}$, where $w = 1/\sigma^2(F_o)$.

Scheme 1. Synthesis for the 1,2-Bis(2-pyridyl)ethane Moiety with Substituents at the 6-Position

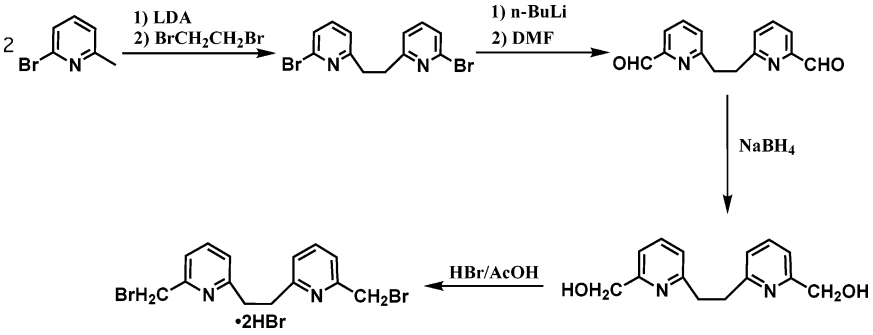

scans from −20.0 to 28.0° in 0.3° step, at $\omega = 90.0°$ and $\chi = 90.0°$. The detector swing angle was 19.91°. A further sweep was performed using ω scans from −20.0 to 28.0° in 0.3° steps, at $\omega = 90.0°$ and $\chi = 180.0°$. The detector swing angle was 19.91°. An additional sweep was performed using ω scans from −20.0 to 28.0° in 0.3° steps, at $\omega = 90.0°$ and $\chi = 270.0°$. The detector swing angle was 19.91°. The crystal-to-detector distance was 45.02 mm. Readout was performed in the 0.137 mm pixel mode. No decay correction was applied. All five structures were solved by direct methods (SIR 92 and SHELEXS 97) and expanded using Fourier techniques. All non-hydrogen atoms were refined anisotropically. Hydrogen atoms were included but not refined. The function minimized was $\sum w(|F_o| - |F_c|)^2$ with $w = 1$. The neutral atom scattering factors were taken from Cromer and Waver.[14] Anomalous dispersion effects were included in F_c,[15] the values for $\Delta f'$ and $\Delta f''$ being taken from reference 16 and those for the mass-attenuation coefficients.[16] Calculations were performed using the Crystal Structure Crystallographic software package.[17] Crystal parameters and important data collection for **1**−**4** are summarized in Table 1. The following information is available in the Supporting Information: a packing diagram of the unit cell, a complete set of crystallographic tables including positional parameters, anisotropic thermal factors, and bond lengths and bond angles.

Results and Discussion

Preparation of Ligands L1−L3. 1,2-Bis(2-formyl-6-pyridyl)ethane and 1,2-bis(2-(bromomethyl)-6-pyridyl)ethane are key synthetic intermediates for the preparation of L1−L3. These intermediates are generally useful in the preparation of multidentate ligands possessing a 1,2-bis(2-pyridyl)ethane moiety. 1,2-Bis(2-formyl-6-pyridyl)ethane can be readily converted to Schiff's bases by reaction with primary and secondary amines, which can subsequently be reduced to amino groups. The amino groups can also be introduced to 1,2-bis(2-(bromomethyl)-6-pyridyl)ethane by substitution reactions with various amines. With previously reported synthetic methods, however, it has been difficult to obtain these synthetic intermediates given the low yields and the many reaction steps required.[13] In an effort to solve this problem, we developed new synthetic routes for the preparation of these synthetic intermediates.

The new synthetic routes are shown in Scheme 1. In a previously published method concerning the preparation of 1,2-bis(2-formyl-6-pyridyl)ethane, 7-(7-triazolopyridine−CH_2−CH_2−) was oxidized with selenium dioxide and resulted in a yield of 40%.[13a] In our method, 1,2-bis(2-formyl-6-pyridyl)ethane was obtained from 1,2-bis(2-bromo-6-pyridyl)ethane by lithiation and formylation using *n*-butyllithium and dry DMF with a yield of 86%. 1,2-Bis(2-bromo-6-pyridyl)ethane was prepared from 2-bromo-6-picoline by a coupling reaction, where 2-bromo-6-picoline was deprotonated with LDA and the resultant carboanion was homocoupled upon addition of 1,2-dibromoethane to afford 1,2-bis(2-bromo-6-pyridyl)ethane in good yield. This method was originally reported by Lehn.[7a] The selective formation of 1,2-bis(2-bromo-6-pyridyl)ethane is probably due to predominant lithiation of the methyl group of 2-bromo-6-picoline but not

(14) Cromer, D. T.; Waber, J. T. *International Tables for X-ray Crystallography*; Kynoch Press: Birmingham, U.K., 1974; Vol. 4.
(15) Ibers, J. A.; Hamilton, W. C. *Acta Crystallogr.* **1964**, *17*, 781.
(16) Creagh, D. C.; McAuley, W. J. *International Tables for X-ray Crystallography*; Kluwer: Boston, MA, 1992.
(17) *Crystal structure analysis package*, version 3.6; Molecular Structure Corp. and Rigaku Corp.: The Woodlands, TX, 2004.

Scheme 2. Syntheses of Tetradentate Ligands L1 and L2

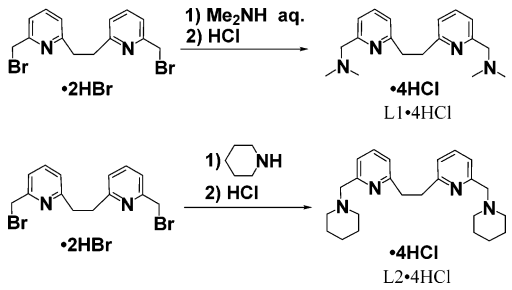

Scheme 3. Synthesis of Hexadentate Ligand L3

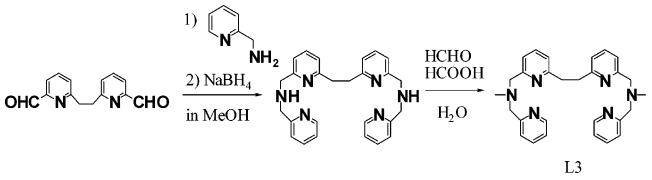

of the bromo group. Using *n*-butyllithium in place of LDA, however, the bromo group was lithiated quantitatively. This is why LDA was used for the coupling reaction and *n*-butyllithium was used for the formylation of 1,2-bis(2-bromo-6-pyridyl)ethane. Thus, our method has advantages over those previously published, not only in terms of the total yield of 1,2-bis(2-formyl-6-pyridyl)ethane but also in relation to the fact that the starting material, 2-bromo-6-picoline, is readily available. The previous method describing the preparation of 1,2-bis(2-(bromomethyl)-6-pyridyl)ethane required eight reactions using 2,6-lutidine as a starting material, and the total yield was less than 1%.[13b] With our method, 1,2-bis(2-(bromomethyl)-6-pyridyl)ethane was readily obtained from 1,2-bis(2-formyl-6-pyridyl)ethane, via reduction with $NaBH_4$ and successive bromination with HBr/AcOH as shown in Scheme 1, and the yield of the product was almost quantitative.

In Schemes 2 and 3, the reactions involving attachment of amino groups to both sides of the 1,2-bis(2-pyridyl)ethane moiety are shown. L1 and L2 were obtained by substitution reactions of the bromo groups of 1,2-bis(2-(bromomethyl)-6-pyridyl)ethane using excess amounts of dimethylamine and piperidine, respectively, in reasonable yields. For the preparation of L3, 1,2-bis(2-formyl-6-pyridyl)ethane was converted to 1,2-bis(2-((methyl(pyridylmethyl)amino)methyl)-6-pyridyl)-ethane via Schiff's base formation upon reaction with 2-pyridylmethylamine and a successive one-pot reduction with $NaBH_4$. The secondary amino groups of 1,2-bis(2-((methyl(pyridylmethyl)amino)methyl)-6-pyridyl)ethane were methylated by Eschweiler−Clarke methylation to afford L3. The yield of L3 from the synthetic intermediate 1,2-bis(2-formyl-6-pyridyl)ethane was 77%. The total yield of L1−L3 was 40−60% from the starting material, 2-bromo-6-picoline. The present synthetic scheme showed significant improvements relative to previously published synthetic strategies.

Synthesis of Copper(II) Complexes 1−4. The mononuclear copper(II) complexes $[Cu(L1)(Cl)]ClO_4$ (**1**) and $[Cu(L2)(Cl)]ClO_4$ (**2**) were isolated in high yield from the reactions of copper(II) perchlorate with L1·4HCl and L2·4HCl in MeOH, respectively. The chloride ion belonging to the hydrochloride salts of the ligands was incorporated into the products. It is known that the tetradentate ligand L4 (see Chart 1), which has a common 1,2-bis(2-pyridyl)ethane moiety, forms both mononuclear and dinuclear copper(II) complexes.[4,5] In the reported results, using a $Cu(OAc)_2$: L4 ratio of 2:1, a μ-acetato-bridged dinuclear copper(II) complex was isolated as a minor product along with the mononuclear complex. In an effort to synthesize a dinuclear complex with L 1 or L2, similar reactions using a $Cu(OAc)_2$:L1 (or L2) ratio of 2:1 were carried out, but no dinuclear complex was isolated. To investigate the chemical species generated in the reaction, FAB mass spectra were determined of aliquots taken from the reaction mixture. These data showed peaks corresponding to the mononuclear complex. No peak corresponding to dinuclear species appeared, even following the addition of mono- and diphenyl phosphate as bridging ligands. Thus, it seems that L1 and L2 prefer to adopt a mononuclear structure and do not serve as dinucleating ligands suitable for incorporation of phosphate esters.

The dinuclear copper(II) complex $[Cu_2(L3)((PhO)_2PO_2)_2](ClO_4)_2$ (**3**) was readily obtained in a high yield by addition of $Na(PhO)_2PO_2$ to a mixture of $Cu(ClO_4)_2$ and L3 in MeOH. The reaction using a $Cu(ClO_4)_2$: L3 ratio of 2:1 was followed by FAB MS. In the absence of a bridging ligand, a mononuclear species $[CuL3]^+$ was detected as a main peak, and upon addition of $(PhO)_2PO_2^-$, new peaks appeared at *m*/*z* 1076 and 827 corresponding to $[L3 + 2Cu + 2(PhO)_2PO_2]^+$ and $[L3 + 2Cu + (PhO)_2PO_2]^+$, respectively. This indicated that L3 binds two Cu ions with incorporation of the phosphate diester as bridging ligands.

In an effort to synthesize a dinuclear complex bridged by a phosphate monoester, $Na_2(PhO)PO_3$ was added to a mixture of $Cu(ClO_4)_2$ and L3 in MeOH, but this afforded the hexanuclear copper(II) complex $[Cu_6(L3)_3((PhO)PO_3)_4](ClO_4)_4$ (**4**). The FAB mass spectrum of **4** showed three strong fragment peaks at *m*/*z* 945, 923, and 750 corresponding to $[L3 + 2Cu + 2(PhO)PO_3 + Na]^+$, $[L3 + 2Cu + 2(PhO)PO_3 + H]^+$, and $[L3 + 2Cu + (PhO)PO_3]^+$, respectively. These fragment peaks commonly include one L3, two Cu ions, and one or two phosphate monoester dianions $(PhO)PO_3^{2-}$ to form a dinuclear unit. The structure of **4** in solution was investigated using cold-spray ionization (CSI) mass spectrometry. The CSI mass spectrum shows the parent peak at *m*/*z* 2724.9 corresponding to $[M - ClO_4]^+$ as a relatively strong peak and a peak at *m*/*z* 1085.9 corresponding to $[L3 + 3Cu + 2(PhO)PO_3 + ClO_4]^+$ as the strongest fragment peak as shown in Figure 2. These data indicated that the hexanuclear structure of **4** is kept in solution and that L3 stabilizes the dinuclear unit.

Thus, L3 stabilizes the various dinuclear units by incorporation of the phosphate esters as bridging ligands, although no dinuclear complex was obtained with L1 and L2. This difference is due to the difference in the pendant groups in L1−L3. The pendant group of L3 may form a tridentate chelate, while the pendant groups of L1 and L2 form bidentate chelates. These chelates differ from each other in terms of their structures and stability. Thus, the structure and

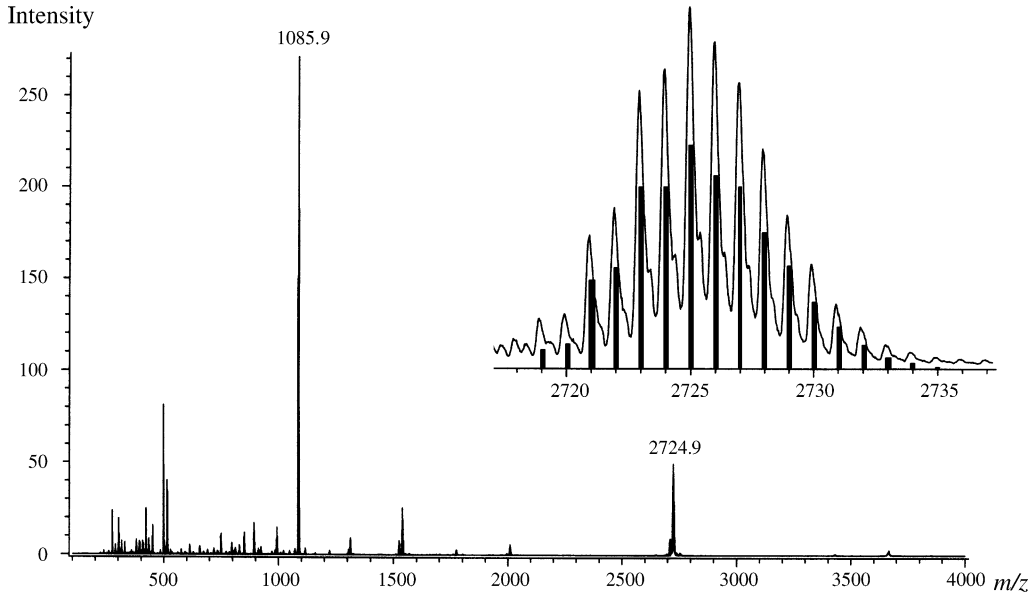

Figure 2. CSI-MS spectrum of $[Cu_6(L3)_3((PhO)PO_3)_4](ClO_4)_4$ (**4**) obtained at −30 °C in MeCN. The isotope pattern of $\{[Cu_6(L3)_3((PhO)PO_3)_4](ClO_4)_3\}^+$ is shown in the spectra.

stability of the copper chelates may be one key factor that determines whether L1−L3 can form the dinuclear unit. This is consistent with the fact that the hexapyridine ligands stabilize the dinuclear complexes with the tridentate pendant groups. This suggests that the tridentate pendant group in this type of polypyridine ligand is more suitable than the bidentate group for the formation of dinuclear structures.

Crystal Structures. Crystal structures of **1**−**4** were determined by X-ray analysis. The structural studies revealed that the common 1,2-bis(2-pyridyl)ethane moiety of L1−L3 adopts various structures given the structural flexibility and that the nuclearity of **1**−**4** is dependent upon not only the pendant groups of L1−L3 but also the bridging ligands. Two N atoms of the 1,2-bis(2-pyridyl)ethane moiety in the mononuclear complexes **1** and **2** bind a Cu ion in a chelate mode to form a seven-membered ring, where two bidentate pendant groups of L1 and L2 bind a Cu ion in a bis-chelate mode. Two N atoms of the same moiety in the dinuclear units of **3** and **4** coordinate to two Cu ions in a syn- or anti-mode, where two tridentate pendant groups of L3 bind two Cu ions in chelate modes. Diphenyl phosphate monoanion $(PhO)_2PO_2^-$ bridges two Cu ions in a μ-1,3 mode to stabilize the dinuclear structure of **3**. Monophenyl phosphate dianion $(PhO)PO_3^{2-}$ bridges three Cu ions in a μ_3-1,3 mode, leading to the hexanuclear structure of **4**.

ORTEP views of **1** and **2** are shown in Figure 3 together with the atomic numbering schemes. Selected bond distances and angles of **1** and **2** are shown in Table 2. Each asymmetric unit of **1** and **2** consists of one cation $[Cu(L)(Cl)]^+$ (L = L1 and L2) and a perchlorate ion, and for **2**, an acetonitrile molecule is present as a crystal solvent. The structures of **1** and **2** are almost identical, indicating that the different substituent groups at the tertiary amino N atoms do not significantly affect the copper coordination structures. Each of the Cu ions in **1** and **2** assumes a five-coordinate structure with two pyridyl N atoms, two N atoms of the tertiary alkylamines, and a Cl^- anion, where the 1,2-bis(2-pyridyl)-ethane moiety forms a seven-membered chelate ring and the two $-PyCH_2NR_2$ pendant groups chelate the Cu ion in a bidentate mode. The coordination geometry was estimated from the τ values. The τ values vary from 0, for an idealized square pyramid, to 1, for an idealized trigonal bipyramid.[18] On the basis of the τ values, 0.25 for **1** and 0.33 for **2**, the

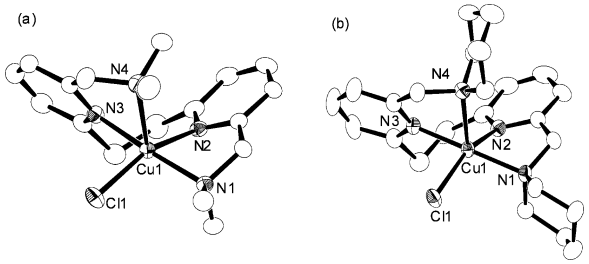

Figure 3. ORTEP diagrams of the cationic portions of (a) [Cu(L1)(Cl)]-(ClO_4) (**1**) and (b) $[Cu(L2)(Cl)](ClO_4)$ (**2**) (ORTEP plot; unlabeled open ellipsoids represent carbon atoms).

Table 2. Selected Bond Distances (Å) and Angles (deg) for **1** and **2**

1		**2**	
Cu1−Cl1	2.2613(7)	Cu1−Cl1	2.285(1)
Cu1−N1	2.025(2)	Cu1−N1	2.093(3)
Cu1−N2	2.082(2)	Cu1−N2	2.035(3)
Cu1−N3	2.001(2)	Cu1−N3	1.988(3)
Cu1−N4	2.361(2)	Cu1−N4	2.350(3)
Cl1−Cu1−N1	94.27(6)	Cl1−Cu1−N1	95.21(8)
Cl1−Cu1−N2	158.84(4)	Cl1−Cu1−N2	152.95(9)
Cl1−Cu1−N3	91.31(6)	Cl1−Cu1−N3	88.65(9)
Cl1−Cu1−N4	96.35(6)	Cl1−Cu1−N4	102.21(9)
N1−Cu1−N2	80.07(8)	N1−Cu1−N2	79.5(1)
N1−Cu1−N3	173.65(9)	N1−Cu1−N3	172.8(1)
N1−Cu1−N4	104.61(8)	N1−Cu1−N4	107.4(1)
N2−Cu1−N3	93.64(9)	N2−Cu1−N3	94.3(1)
N2−Cu1−N4	104.80(8)	N2−Cu1−N4	104.7(1)
N3−Cu1−N4	77.73(8)	N3−Cu1−N4	77.6(1)

(18) Addison, A. W.; Rao, T. N.; Reedijk, J.; Rijin, J. V.; Verschoor, G. C. *J. Chem. Soc., Dalton Trans.* **1984**, 1349.

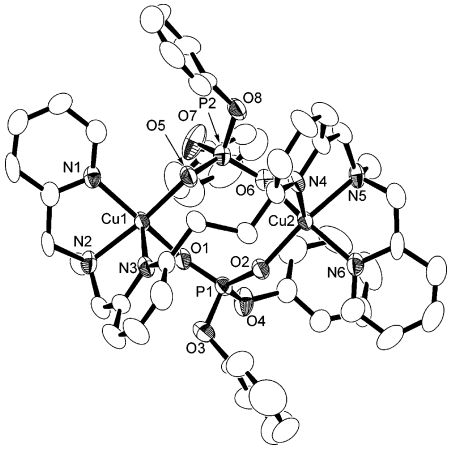

Figure 4. ORTEP diagram of the cationic portion of $[Cu_2(L3)(Ph_2PO_4)_2](ClO_4)_2$ (**3**) (ORTEP plot; unlabeled open ellipsoids represent carbon atoms). Hydrogen atoms have been omitted.

coordination geometries represent distorted square pyramids. Three short Cu−N bonds and the Cu−Cl bond form the basal plane of the square pyramid with N1, N2, N3, and Cl1. The Cu−N bond with N4 in the apical position is significantly longer (see Table 2).

The related tetradentate ligand L4 (see Chart 1) forms a mononuclear copper(II) complex $[Cu(L4)]^{2+}$ with a tetrahedrally distorted four-coordinate structure,[4] different from the five-coordinate structures of **1** and **2**. The tetrahedral distortion is caused by steric repulsion between the bipyridine pendant groups of L4. The steric repulsion may destabilize the bis-chelate structure in the mononuclear complex, leading to formation of the dinuclear complex with L4. In the sterically hindered tetradentate ligands L5 and L6, two methyl groups are substituted at the α-positions of the N atoms of the pendant groups. Since the steric repulsion between the pendant groups is enhanced by the methyl groups, L5 and L6 form dinuclear Cu(I) complexes with double-strand helix structures where steric repulsion is minimized.[7] Although L1 and L2 are tetradentate ligands similar to L4−L6 possessing a common 1,2-bis(2-pyridyl)-ethane moiety, the pendant groups of L1 and L2 have more flexible structures than the bipyridines and phenanthroline of L4−L6. The flexible pendant groups of L1 and L2 allow for the formation of five-coordinate structures in **1** and **2**, where there is no steric repulsion between the pendant groups in the five-coordinate structures. Therefore, it may be concluded that L1 and L2 specifically stabilize the mononuclear structures given the flexible pendant groups.

The ORTEP view of **3** is shown in Figure 4 together with the atomic numbering schemes. Selected bond distances and angles of **3** are given in Table 3. The asymmetric unit of **3** consists of one dication $[Cu_2(L3)((PhO)_2PO_2)_2]^{2+}$ and two perchlorate ions. Two N atoms of the 1,2-bis(2-pyridyl)-ethane moiety in L3 coordinate to two Cu ions in a syn-mode. Each Cu ion is bound by a pendant group, a $-PyCH_2N(CH_3)CH_2Py$ moiety of L3, in an end-capping tridentate chelate mode and bridged by two $(PhO)_2PO_2^-$ monoanions in a μ-1,3 mode and, thus, pentacoordinated with three N atoms of the tridentate pendant group and two O atoms of the two $(PhO)_2PO_2^-$ bridges. The coordination geometries of the Cu ions are distorted square pyramidal, based on the τ values,[18] 0.22 and 0.33. Each equatorial plane is formed by two N atoms and two O atoms. The equatorial Cu−N and Cu−O bond lengths are normal (1.935−2.031 Å) (see Table 3). Each apical position is occupied by a N atom with a Cu−N bond significantly longer (2.221 and 2.261 Å for two Cu ions) than the equatorial ones. The geometries and bond lengths around the P atoms are similar to those of the free phosphate diesters.[19] The Cu···Cu distance is 4.812 Å. The metal−metal distances in dinuclear metalloenzymes that bind phosphate esters range from ca. 3 to 5 Å. The metal−metal distances in polynuclear metal complexes bridged by the O−P−O bridges range from 2.9 to 5.5 Å.[11,12] Shorter distances are observed in the dinuclear complexes with one or more additional single atom bridges, and longer ones in those with only O−P−O bridges. For example, the Ni···Ni distances in a dinuclear Ni(II) complex bridged by two O−P−O bridges, where each Ni ion is bound by a mononucleating macrocyclic ligand, are 4.863, 5.424, and 5.116 Å.[20] The Cu···Cu distance of 4.812 Å in **3** is slightly shorter than the metal−metal distances reported for the dimetal centers linked by only O−P−O bridges. This indicated that the hexadenate ligand L3 may have facilitated the reduction in the Cu···Cu distance.

Table 3. Selected Bond Distances (Å) and Angles (deg) for **3**

Cu1···Cu2	4.812(1)	Cu1−O1	2.031(6)	Cu1−O5	1.935(6)
Cu1−N1	1.999(7)	Cu1−N2	2.016(8)	Cu1−N3	2.221(8)
Cu2−O2	1.949(6)	Cu2−O6	1.989(6)	Cu2−N4	2.261(7)
Cu2−N5	2.032(8)	Cu2−N6	2.002(8)		
O1−Cu1−O5	92.1(2)	O1−Cu1−N1	153.5(3)	O1−Cu1−N2	91.4(3)
O1−Cu1−N3	95.9(3)	O5−Cu1−N1	92.7(3)	O5−Cu1−N2	173.5(3)
O5−Cu1−N3	105.1(3)	N1−Cu1−N2	81.8(3)	N1−Cu1−N3	107.9(3)
N2−Cu1−N3	80.0(3)	O2−Cu2−O6	90.8(3)	O2−Cu2−N4	109.7(2)
O2−Cu2−N5	170.3(3)	O2−Cu2−N6	91.5(3)	O6−Cu2−N4	94.2(3)
O6−Cu2−N5	91.4(3)	O6−Cu2−N6	157.0(3)	N4−Cu2−N5	79.5(3)
N4−Cu2−N6	106.4(3)	N5−Cu2−N6	82.8(3)		

Compound **4** crystallizes in the monoclinic space group *C*2/*c* with half of the molecule in the asymmetric part of the unit cell. The core structure of **4** is shown in Figure 5 together with the atomic numbering schemes. Selected bond distances and angles of **4** are shown in Table 4. **4** has a hexanuclear core $[Cu_6(L3)_3(PhOPO_3)_4]^{4+}$ that consists of one $[Cu_2(L3)]^{4+}$ unit and two $[Cu_2(L3)(PhOPO_3)_2]$. Within the $[Cu_2(L3)(PhOPO_3)_2]$ unit, two Cu ions are bridged by two $PhOPO_3^{2-}$ dianions in a μ-1,3-O−P−O mode. Thus, one of three coordinative O atoms in the $PhOPO_3^{2-}$ dianion is free from coordination in the $[Cu_2(L3)(PhOPO_3)_2]$ unit and coordinates to one Cu ion in the $[Cu_2(L3)]^{4+}$ unit, so that the $PhOPO_3^{2-}$ dianion bridges three Cu ions by using the three O atoms in a μ_3-1,3 mode. Two $[Cu_2(L3)(PhOPO_3)_2]$ units are linked by a $[Cu_2(L3)]^{4+}$ unit with four μ_3-$PhOPO_3$ bridges to form the hexanuclear core. Two N atoms of the 1,2-bis(2-pyridyl)-ethane moiety of L3 coordinate to two Cu ions in a syn-

(19) (a) Ezra, F. S.; Collin, R. C. *Acta Crystallogr.* **1973**, *B29*, 1398. (b) Giarda, L.; Garbassi, F.; Calcaterra, M. *Acta Crystallogr.* **1973**, *B29*, 1826.

(20) Santana, M. D.; Garcia, G.; Lozano, A. A.; López, G.; Tudela, J.; Perez, J.; Garcia, L.; Lezama, L.; Rojo, T. *Chem.—Eur. J.* **2004**, *10*, 1738.

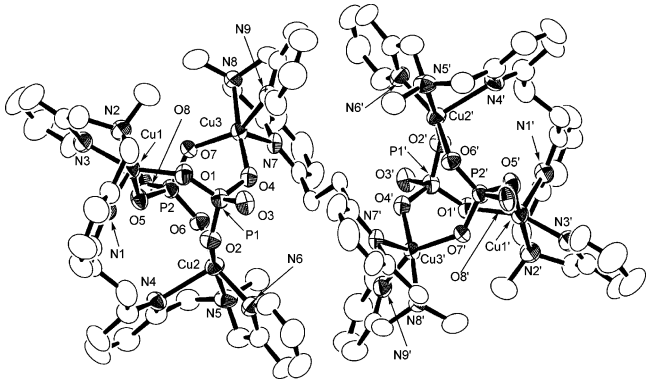

Figure 5. ORTEP diagram of the cationic portion of $[Cu_6(PhPO_4)_4(L3)_3](ClO_4)_4$ (**4**) (ORTEP plot; unlabeled open ellipsoids represent carbon atoms). Hydrogen atoms and phenyl ring of μ-$PhPO_4$ have been omitted.

Table 4. Selected Bond Distances (Å) and Angles (deg) for **4**

Cu1···Cu2	4.710(2)	Cu1···Cu3	4.188(2)	Cu2···Cu3	4.644(2)
Cu1−O1	1.930(6)	Cu1−O5	1.928(6)	Cu1−N1	2.017(8)
Cu1−N2	2.057(8)	Cu1−N3	2.286(8)	Cu2− O2	1.931(6)
Cu2−O6	1.943(6)	Cu2−N4	2.320(8)	Cu2−N5	2.078(8)
Cu2−N6	2.003(7)	Cu3−O4	1.910(6)	Cu3−O7	1.966(6)
Cu3−N7	2.042(8)	Cu3−N8	2.047(8)	Cu3−N9	2.257(8)

O1−Cu1−O5	96.9(3)	O1−Cu1−N1	159.0(3)	O1−Cu1−N2	86.9(3)
O1−Cu1−N3	90.8(3)	O5−Cu1−N1	92.9(3)	O5−Cu1−N2	172.5(3)
O5−Cu1−N3	108.1(3)	N1−Cu1−N2	81.5(3)	N1−Cu1−N3	103.7(3)
N2−Cu1−N3	78.3(3)	O2−Cu2−O6	96.7(3)	O2−Cu2−N4	108.1(3)
O2−Cu2−N5	172.0(3)	O2−Cu2−N6	90.5(3)	O6−Cu2−N4	95.3(3)
O6−Cu2−N5	89.6(3)	O6−Cu2−N6	156.2(3)	N4−Cu2−N5	76.1(3)
N4−Cu2−N6	104.0(3)	N5−Cu2−N6	81.8(3)	O3−Cu3−O7	98.2(3)
O3−Cu3−N7	91.7(3)	O3−Cu3−N8	172.6(3)	O3−Cu3−N9	103.7(3)
O7−Cu3−N7	148.8(3)	O7−Cu3−N8	88.7(3)	O7−Cu3−N9	94.7(3)
N7−Cu3−N8	81.0(3)	N7−Cu3−N9	111.7(3)	N8−Cu3−N9	78.3(3)

mode for the $[Cu_2(L3)(PhOPO_3)_2]$ unit and in an anti-mode for the $[Cu_2(L3)]$ unit. Each Cu ion in **4** is pentacoordinated with three N atoms of the tridentate pendant group and two O atoms of the two $PhOPO_3^{2-}$ dianions. The coordination of the Cu ions in the $[Cu_2(L3)(PhOPO_3)_2]$ unit represent distorted square pyramidal geometries, based on the τ values,[18] 0.23 and 0.26. The coordination geometry of the Cu ion in the $[Cu_2(L3)]^{4+}$ unit is largely distorted (τ value[18] = 0.40). All bond distances around the Cu ions in **4** are normal for these coordination geometries (see Table 4). The geometries and bond lengths around the P atoms are similar to those of the free phosphate monoesters.[21] The Cu···Cu distances are Cu1···Cu2 = 4.710 Å, Cu1···Cu3 = 4.188 Å, and Cu2···Cu3 = 4.644 Å. The Cu1···Cu3 distance of 4.188 Å is quite short for dinuclear centers bridged only by phosphate esters in the μ-1,3-O−P−O mode. As indicated above, these values are often greater than 5 Å. It is noted that the Cu1···Cu3 distance is similar to the Zn···Zn distance of 3.94 Å in phosphate-modified alkaline phosphatase.[10a] The Cu···Cu distance in the $[Cu_2(L3)(PhOPO_3)_2]$ unit is 4.710 Å, being shorter than 4.812 Å in **3**, indicating that the electronic repulsion between the Cu(II) ions was more effectively reduced by the phosphate monoester dianions than by the phosphate diester monoanions.

The crystal structure of **3** revealed that the tridentate pendant group of L3 adopts an end-capping chelate coordination mode, which leaves two empty coordination sites in a cis arrangement, favorable for approximately two equivalent μ-O−P−O bridges. It was also shown that the μ-O−P−O bridge from the phosphate diester anions specifically stabilizes the dinuclear structure of **3**, where two donor O atoms in the diphenyl phosphate anion are sufficient to bridge two Cu ions. Thus, both the pendant group of L3 and the bridging ligand are responsible for the dinuclear structure of **3**. Although a phosphate monoester dianion with three donor O atoms can potentially bridge three metal ions, examples of trinuclear complexes bridged by phosphate monoester dianions are quite few due to difficulties relating to the formation of trinuclear structures.[22] To the best of our knowledge, **4** is the first example representing the structural characterization of a hexanuclear complex bridged by phosphate monoester dianions. Recently, it was reported that a hexanuclear copper(II) complex with a NO_3 bridge was obtained with a new octadentate polypyridine ligand.[23] In **4**, two $[Cu_2(L3)(PhOPO_3)_2]$ units are linked by a $[Cu_2(L3)]^{4+}$ unit with four μ_3-1,3-$PhOPO_3$ bridges. The anti-coordination mode of the 1,2-bis(2-pyridyl)ethane moiety in the $[Cu_2(L3)]^{4+}$ unit makes it possible for each Cu ion of the $[Cu_2(L3)]^{4+}$ unit to participate at each trinuclear center. Thus, the μ_3-1,3-$PhOPO_3$ bridges and the flexible structure of the 1,2-bis(2-pyridyl)ethane moiety facilitated the formation of the hexanuclear structure of **4**. Therefore, it is concluded that L3 is a promising ligand that can form, in addition to various dinuclear units, the unique hexanuclear complex by accumulation of the dinuclear units via incorporation of phosphate esters as bridging ligands.

Hydrolysis of Tris(*p*-nitrophenyl) Phosphate, TNP. To evaluate biological relevance of the Cu(II) complexes of the present ligands, the hydrolysis of tris(*p*-nitrophenyl) phosphate (TNP) was kinetically investigated. For these reactions, the mononuclear Cu(II) complex of L2, **2**, and the dinuclear Cu(II) complex of L3 were used. The dinuclear Cu(II) complex of L3 was prepared by mixing L3 and $Cu(ClO_4)_2 \cdot 6H_2O$ (1:2, mol/mol) in 30% MeCN−H_2O at various pH values (see Experimental Section). The positive mode and negative mode CSI mass spectra of the dinuclear Cu(II) complex of L3 are shown in Figure 6A,B, respectively. The positive mode spectrum at pH 7.0 shows a major peak at *m*/*z* 793 corresponding to $\{[Cu_2(L3)(OH)](ClO_4)_2\}^+$, and those at pH > 8.0 a major peak at *m*/*z* 711 corresponding to $\{[Cu_2(L3)(OH)_2](ClO_4)\}^+$. Any peaks assignable to free ligand or to mononuclear copper complex were not detected at all. These results clearly show that L3 forms the dinuclear complexes quantitatively when 2 equiv of $Cu(ClO_4)_2 \cdot 6H_2O$ was added to L3 at pH 7.0−10.0 in aqueous solution. The

(21) (a) Garbassi, F.; Giavda, L.; Fagherazzi, G. *Acta Crystallogr.* **1972**, *B28*, 1665. (b) Klooster, W. T.; Craven, B. M. *Acta Crystallogr.* **1992**, *B48*, 19. (c) Reinoso, S.; Uitoria, P.; Vgalde, M.; Gutierrez-Zorrilla, J. M.; Luque, A.; Roman, P. *Acta Crystallogr.* **1999**, *C55*, 683. (d) McDonald, W. S.; Cruiokshank, D. W. J. *Acta Crystallogr.* **1971**, *B27*, 1315.

(22) (a) Kimura, E.; Aoki, S.; Koike, T.; Shiro, M. *J. Am. Chem. Soc.* **1997**, *119*, 3068. (b) Fry, F. H.; Jensen, P.; Kepert, C. M.; Spiccia, L. *Inorg. Chem.* **2003**, *42*, 5637.

(23) de Hoog, P.; Gamez, P.; Lüken, M.; Roubeau, O.; Krebs, B.; Reedijk, J. *Inorg. Chim. Acta* **2004**, *357*, 213.

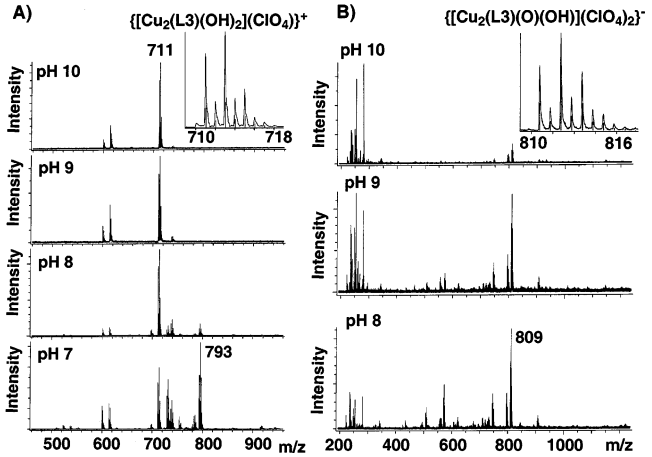

Figure 6. CSI mass spectra, (A) positive mode and (B) negative mode, of a mixture of L3 and $Cu(ClO_4)_2$ (1:2, mol/mol) in 30% MeCN−H_2O (v/v) at various pH values. The pH was adjusted by addition of NaOH. Insert: Isotope patterns of mass peaks at *m*/*z* 711 for $\{[Cu_2(L3)(OH)_2](ClO_4)\}^+$ and at *m*/*z* 809 for $\{[Cu_2(L3)(OH)_3](ClO_4)_2\}^-$ are shown, and calculated isotope patterns are represented by bars under each peak cluster.

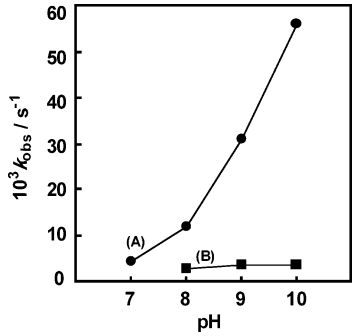

Figure 7. Plot of k_{obs} vs pH for the Cu^{II}-mediated hydrolysis of tris(*p*-nitrophenyl) phosphate (TNP): (A) dinuclear Cu(II) complex prepared by mixing L3 and 2 equiv of $Cu(ClO_4)_2 \cdot 6H_2O$ (circles); (B) mononuclear Cu(II) complex **2** (squares). Reaction conditions: [complex] = 2.0 mM; [TNPP] = 20 μM; 20 mM buffer (HEPES (pH 7), TAPS (pH 8), CHES (pH > 9)); 35 °C; I = 0.10 M ($NaClO_4$) in 30% MeCN−H_2O solution.

pH dependence of the pseudo-first-order rate constants k_{obs} for the TNP hydrolysis with the dinuclear Cu(II) complex of L3 prepared as above and with the mononuclear Cu(II) complex **2** over the pH range 7.0−10.0 (four different points) is shown in Figure 7A,B, respectively. The dinuclear complex of L3 largely accelerated the TNP hydrolysis at pH 8.0−10.0, and the k_{obs} values increased with increasing the pH. The k_{obs} values for **2**, however, were almost constant, (3.09−3.72) × 10^{-3} s^{-1}, at pH 8.0−10.0, and the acceleration is only by 3-fold as compared with k_0 values, (1.20−1.30) × 10^{-3} s^{-1}, at pH 7.0−10.0, for the TNP hydrolysis only by using buffer and OH^- ions (blank experiments). The reactions were also carried out by addition of only L3 ligand or $Cu(ClO_4)_2$ to the blank experiments, and the rate constants are 1.24 × 10^{-3} or 1.30 × 10^{-3} s^{-1} at pH 9.0, respectively, almost the same as the k_0 values. These results show that the dinuclear Cu(II) complex of L3 specifically accelerates the TNP hydrolysis.

The potentiometric pH titration curve of the dinuclear Cu(II) complex of L3 is shown in Figure 8. The pH was increased stepwise upon addition of NaOH; 1, 2, 3, and 4 equiv of OH^- ions were consumed at pH 6.0, 7.5, 9.0, and

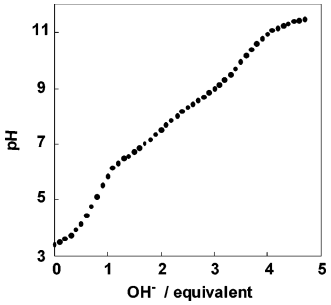

Figure 8. Potentiometric pH titration curve of the dicopper(II) complex of L3 at 25 °C. The pH was measured when an aqueous solution of NaOH ([NaOH] = 0.1 M) was added dropwise to a solution (30% MeCN−H_2O (v/v)) of the mixture of L3 and $Cu(ClO_4)_2$ (1:2, mol/mol, [complex] = 1 mM) at I = 0.1 M ($NaClO_4$).

11, respectively, indicating that 1, 2, 3, and 4 equiv of OH^- ions are incorporated into the $[Cu_2(L3)]^{4+}$ complex so that four different dinuclear Cu(II) complexes are formed. Three major species were detected from the CSI mass spectra (Figure 6) with the pH change. At pH 7.0, the positive mode CSI mass spectrum shows a major peak at *m*/*z* 793 corresponding to $\{[Cu_2(L3)(OH)](ClO_4)_2\}^+$ and a minor peak at *m*/*z* 711 corresponding to $\{[Cu_2(L3)(OH)_2](ClO_4)\}^+$. At the pH > 8.0, the positive mode CSI mass spectra show only one major species at *m*/*z* 711. Interestingly, however, the negative mode CSI mass spectra show a different major peak at *m*/*z* 809 corresponding to $\{[Cu_2(L3)(O)(OH)](ClO_4)_2\}^-$ at pH > 8.0. Three species, $\{[Cu_2(L3)(OH)](ClO_4)_2\}^+$, $\{[Cu_2(L3)(OH)_2](ClO_4)\}^+$, and $\{[Cu_2(L3)(O)(OH)](ClO_4)_2\}^-$, are formed by incorporation of 1, 2, and 3 equiv of OH^- ions into the $[Cu_2(L3)]^{4+}$ complex, respectively. This is consistent with the results of the potentiometric titration, where 3 equiv of OH^- ions was consumed at pH 9.0. These results suggest that the active species for the TNP hydrolysis at pH 8.0 and 9.0 may be $[Cu_2(L3)(O)(OH)]^+$. Two major peaks observed at *m*/*z* 711 and 809 in the positive and negative spectra are decreased at pH 10.0 as compared to those at pH 8.0 and 9.0 (see Figure 6). This indicates that the amount of $[Cu_2(L3)(O)(OH)]^+$ is decreased and a new dinuclear Cu(II) complex incorporating 4 equiv of OH^- ions, $[Cu_2(L3)(O)(OH)_2]$, is generated at pH 10.0, but the latter species is not detected by the CSI mass spectra probably due to the neutral charge and/or the instability. Since the TNP hydrolysis was further greatly accelerated at pH 10.0, a dinuclear Cu(II) complex incorporating 4 equiv of OH^- ions, $[Cu_2(L3)(O)(OH)_2]$, might be a more active species for the TNP hydrolysis.

The apparent second-order rate constants k_2 derived as $k_{obs} - k_0$/[total Cu^{II} complex] are shown in Table 5 together with the reported second-order rate constants for the metal-complex-promoted TNP hydrolysis under aqueous conditions. The chemical structures of mononucleating and dinucleating ligands reported for the TNP hydrolysis are shown in Chart 3. The k_2 values obtained for the dinuclear Cu(II) complex of L3 are the highest values at pH 7.0−10.0 in the reported ones, clearly indicating that the dinuclear Cu(II) complex of L3 is one of the most active system for the TNP hydrolysis.

Table 5. Second-Order Rate Constants for the TNP Hydrolysis Promoted by Metal Complexes in Aqueous Solutions

	$k_2/M^{-1}\,s^{-1}$				
complex	pH 7	pH 8	pH 9	pH 10	ref
Cu_2L3	2.32	6.10	15.7	28.1	this work
CuL7	0.3				25
CuL8		0.94			26
Cu_2L9		1.48			26
ZnL10			7.0		27
ZnL11			3.7		27
ZnL12				8.7	28
Zn_2L13				1.5	29
$(ZnL14)_2$				3.2	30

Chart 3. Chemical Structures of Ligands Used for the TNP Hydrolysis

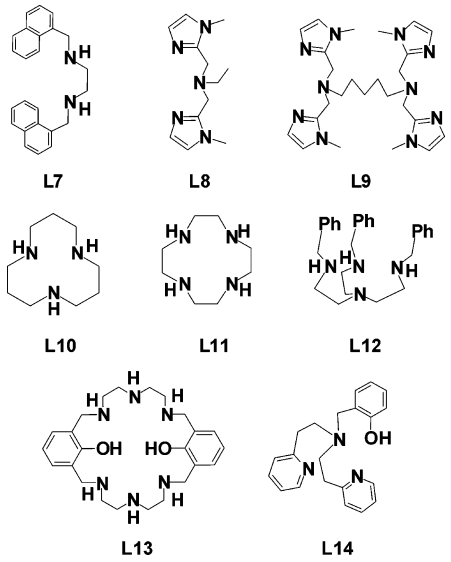

It is shown that the active species may be $[Cu_2(L3)(O)(OH)]^+$ and/or $[Cu_2(L3)(O)(OH)_2]$. Since 3 and 4 equiv of OH^- ions are incorporated in the active species, Lewis acidity of the Cu(II) ions are decreased and the nucleophilicity of the Cu−OH in the active species must be high. That may be the reason the dinuclear Cu(II) complex of L3 shows such a high hydrolytic activity. The most important thing is that the hydrolytic activity of the dinuclear Cu(II) complex of L3 is increased at the relatively higher pH region (pH 9−10). This is similar to the hydrolytic activity of the alkaline phosphatase, where it acts at high pH region (pH 8−9). These results suggest that, for the hydrolysis of phosphate esters, the high nucleophilicity of the active species is necessary. The stable dinuclear structure with the variable Cu−Cu distance is supported by L3 possessing the flexible 1,2-bis(2-pyridyl)ethane moiety and may make it possible to form such a highly nucleophilic active species. Therefore, a ligand capable of incorporating such an active dinuclear core is useful to make a functional model of the alkaline phosphatase. Recently, a good structural Cu(II) model complex for alkaline phosphatase was reported,[24] but the relationship between the hydrolytic activity and the dinuclear structure has not been clarified yet. To answer this question, a new functional model showing high hydrolytic activity may be necessary. Hydrolysis of phosphate diester and monoester with the present system is now under investigation.

Conclusion

Three new polypyridine ligands L1−L3 possessing a common 1,2-bis(2-pyridyl)ethane moiety were efficiently prepared by utilizing novel synthetic routes. These ligands form the Cu(II) complexes **1**−**4** possessing various nuclearity. The crystal structures of **1**−**4** were determined by X-ray analysis, and the structures in solution were investigated by the FAB and CSI mass spectra. L1 and L2 bind a Cu(II) ion with two bidentate pendant groups in a bis-chelate mode to form the mononuclear complexes **1** and **2**, respectively, where the 1,2-bis(2-pyridyl)ethane moiety forms a seven-membered chelate ring. The flexible structure of the bidentate pendant groups facilitated the formation of the five-coordinate structures of **1** and **2**. L1 and L2 specifically stabilize the mononuclear structures of **1** and **2** since the steric repulsion between the pendant groups is reduced in the five-coordinate structure. L3 binds two Cu ions with two tridentate pendant groups in chelate modes to form the various dinuclear units in the dinuclear complex **3** and the hexanuclear complex **4**, where the 1,2-bis(2-pyridyl)ethane moiety of L3 acts as a spacer to separate the two Cu ions by a distance suitable for incorporation of phosphate esters as bridging ligands. To the best of our knowledge, **4** represents the first example of the structural characterization of a hexanuclear complex bridged by phosphate monoester dianions. The Cu···Cu distances in **3** and **4** are slightly shorter than the metal−metal distances of known polynuclear complexes bridged by only μ-O−P−O bridges, indicating that L3 deceases the metal−metal distances. The formation of the polynuclear structures in **3** and **4** is dependent upon the tridentate pendant group and the bridging ligand. L3 represents a promising ligand that can form, in addition to the various dinuclear units, unique hexanuclear complexes by accumulating the dinuclear units with incorporation of phosphate esters as bridging ligands. The dinuclear Cu(II) complex of L3 greatly promotes the hydrolysis of TNP at the relatively higher pH (pH 9−10) in 30% MeCN−H_2O (v/v) solution, and the second-order rate constants k_2 are the largest in the reported k_2 values for the TNP hydrolysis in aqueous media. This may be due to the high nucleophilicity of the Cu−OH in the active species and due to the stable dinuclear structure with the variable Cu−Cu distance supported by L3 possessing the flexible 1,2-bis(2-pyridyl)ethane moiety. This study might contribute to a new functional model of alkaline phosphatase.

(24) Barker, J. E.; Liu, Y.; Martin, N. D.; Ren, T. *J. Am. Chem. Soc.* **2003**, *125*, 13332.
(25) Negi, S.; Schneider, H.-J. *Tetrahedron Lett.* **2002**, *43*, 411.
(26) Clewley, R. G.; Slebocka-Tilk, H.; Brown, R. S. *Inorg. Chim. Acta* **1989**, *157*, 233.
(27) Koike, T.; Kimura, E. *J. Am. Chem. Soc.* **1991**, *113*, 8935.
(28) Ibrahim, M. M.; Shimomura, N.; Ichikawa, K.; Shiro, M. *Inorg. Chim. Acta* **2001**, *313*, 125.
(29) Kong, D.; Martell, A. E.; Reibenspies, J. *Inorg. Chim. Acta* **2002**, *333*, 7.
(30) Adams, H.; Bailey, N. A.; Fenton, D. E.; He, Q.-Y. *J. Chem. Soc., Dalton Trans.* **1996**, 2857.

Acknowledgment. This work was supported by a Grant in-Aid for Scientific Research B (14340210) from the JSPS and with the aid of Doshisha University's Research Promotion Fund.

Supporting Information Available: X-ray crystallographic files in CIF format for **1**−**4**, Tables S1−S16, providing crystallographic experimental details, final atomic coordinates, thermal parameters, and selected bond distances and angles for **1**−**4**, and Figures S1−S12, showing ORTEP diagrams, stereoviews, and packing diagrams of **1**−**4** (PDF). This material is available free of charge via the Internet at http://pubs.acs.org.

IC049240W